

Power Line Enhanced Cooperative Wireless Communications

Marc Kuhn, Stefan Berger, Ingmar Hammerström, and Armin Wittneben

Abstract—In this paper, we investigate the use of power line communication (PLC) to assist cooperative wireless relaying. We consider a communication scheme that uses the power line to initialize and synchronize wireless amplify-and-forward relays and to broadcast information between the relays. Starting from an analysis of transfer functions and noise measurements of PLC channels in office and residential environments, we propose a power line transmission scheme for the inter-relay-communication and assess the influence of this scheme on wireless relaying. This scheme is based on linear precoded orthogonal frequency-division multiplexing; it is designed to optimally exploit the frequency diversity available on PLC channels. The use of PLC leads to a very flexible way of enhancing wireless communications by plugging in additional relays where they are needed—without additional wiring.

Index Terms—Cooperative wireless relaying, linear precoding, multiple-input–multiple-output (MIMO) systems, power line communication (PLC), precoded orthogonal frequency-division multiplexing (OFDM).

I. INTRODUCTION

POWER LINE COMMUNICATION (PLC) offers the possibility to use the well-developed infrastructure of the electrical energy distribution grid for data transmission. For the time being, there is no harmonized international standard for broadband PLC [1]. But IEEE started standardization of PLC physical and MAC layer in June 2005. In Europe, broadband PLC is limited to frequencies between 1 and 30 MHz, because of restrictions regarding electromagnetic compatibility (EMC). Future communication systems are expected to use much higher data rates as today's wireless local area networks (WLANs) [2]. In this paper, we study an approach to boost high data rate wireless communications by using existing power lines in a flexible and cost-efficient way.

In wireless networks, spatial diversity and spatial multiplexing gains are achieved by multiple antennas at the transmitter and at the receiver. Using *cooperative relaying strategies* [3]–[7] these gains are also possible for single-antenna nodes. Spatial multiplexing is mandatory to achieve the high bandwidth efficiency that is necessary for future Gigabit/s wireless communication systems [2]. Practical cooperative

Manuscript received April, 18, 2005; revised December 15, 2005 and February 20, 2006. This paper was presented in part at the Sixth IEEE Workshop on Signal Processing Advances in Wireless Communications, New York, June 5–8, 2005.

The authors are with the Communication Technology Laboratory, Swiss Federal Institute of Technology (ETH) Zurich, CH-8092 Zurich, Switzerland (e-mail: kuhn@nari.ee.ethz.ch; berger@nari.ee.ethz.ch; hammerstroem@nari.ee.ethz.ch; wittneben@nari.ee.ethz.ch).

Digital Object Identifier 10.1109/JSAC.2006.874407

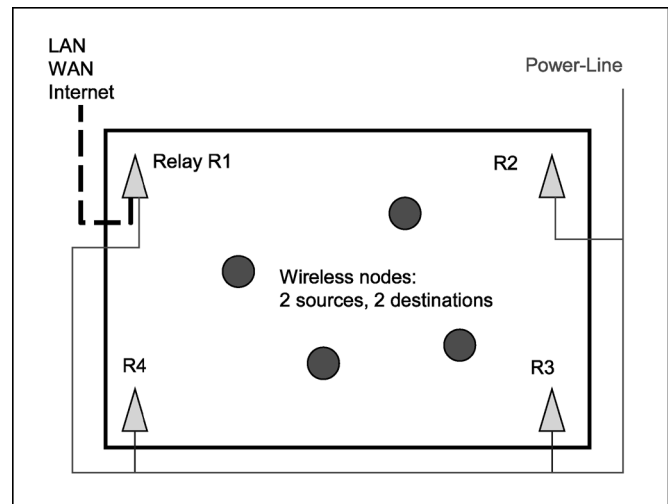


Fig. 1. Scenario: wireless MU-ZFR assisted by PLC between the relays.

relaying schemes for spatial multiplexing gains usually need the exchange of information between the relays.

In this paper, we consider a cooperative relaying scheme with fixed infrastructure amplify-and-forward (AF) relays (support nodes) connected to the power grid for power supply. We study the possibility to use PLC for the considerably high signaling overhead between the wireless relays in such scenarios; some basic ideas to this were first published in [8]. In contrast to our approach, the authors in [9] study the use of cooperative communication for PLC.

The considered scenario is shown in Fig. 1: a room (e.g., a conference room) with nodes that need high-speed wireless data communication; these nodes are mobile, but the velocity is low (less than 5 km/h); an example for such a scenario is a high-speed WLAN. Fixed infrastructure AF relays assist the communication between the wireless nodes (N_r : number of relays). The nodes are equipped with a single antenna. We consider two different traffic patterns.

- 1) *Ad Hoc WLAN*: The wireless nodes form an ad hoc network using orthogonal frequency-division multiplexing (OFDM) under a two-hop relaying scheme. We assume that the wireless nodes can be divided into N_a source/destination pairs; the transmission from a source node to its associated destination node includes two channel uses: one for the *uplink* transmission from the source to all relays and one for the *downlink* transmission when each relay broadcasts an amplified (but not decoded) version of its received signal to the destination nodes.

- 2) *Infrastructure-based WLAN*: One relay is connected to a high data rate backhaul [e.g., wide-area network (WAN), LAN etc., see Fig. 1]. This relay acts as access point (AP) for the wireless nodes. The transmission between the AP and a particular wireless node is again done as described in 1): The AP relay is considered as a new wireless source node and the other relays assist in a two-hop relaying scheme.

In this paper, the AF relay gains are assigned such that the interference between different source/destination links is nulled by coherent combining the broadcasted signals; we refer to this scheme as *multiuser zero-forcing relaying* (MU-ZFR) [7], [10]. This essentially realizes a distributed spatial multiplexing gain with single-antenna nodes, enabling high data rates. Using this scheme, N_a source/destination pairs are orthogonalized in the spatial dimension; if more wireless nodes are involved, MU-ZFR can be combined with an additional multiple-access scheme, e.g., time-division multiple-access (TDMA). For MU-ZFR, all relays have to be synchronous and in an initialization phase every relay has to broadcast its channel state information (CSI) regarding all wireless nodes (uplink and downlink CSI) to all other relays; in [10] is shown, how this information can be acquired. The CSI has to be updated from time to time, because otherwise, it becomes outdated. In the following, we investigate if synchronization and initialization/updates of the wireless relays can be done using PLC.

We assume that every relay is supplied by a power outlet, and therefore the power line can be used for communication between the relays (PLC backbone). In addition, it is also possible to connect one or more relays to the high data rate backhaul over the power line (see Fig. 1); these additional APs do not have a fixed infrastructure-based connection to the backhaul, i.e., high data rate PLC has to be used. The wireless source and destination nodes are not necessarily connected to the power line and communicate only over the wireless medium; they do not cooperate, e.g., there is no joint decoding.

The analysis of the PLC backbone is based on extensive measurements of the transfer function and the noise of the PLC channels—for office and residential environments. The channel capacity of these indoor PLC channels is determined at frequencies between 1 and 30 MHz. A PLC transmission scheme is proposed and the expected jitters are analyzed, because they determine the suitability of PLC for the relay synchronization.

This paper is outlined as follows. In Section II, the results of the PLC measurement campaign and the investigation of the power line channel capacity are given. In Section III, we describe MU-ZFR. In Section IV, a PLC backbone for wireless multiuser zero-forcing is studied; we propose a PLC transmission scheme that is optimized regarding the properties of PLC channels and address the issue of relay synchronization over power line channels.

Notation: The operators \odot , $E_{\{x\}}[\cdot]$, and $(\cdot)^H$ denote the Hadamard (element-wise) product, expectation with respect to x , and conjugate complex transpose, respectively. The terms $\mathbf{X}[i, j]$, $\mathbf{X}[:, i]$, and $\mathbf{X}[i, :]$ denote the element (i, j) , the i th column, and the i th row of a matrix \mathbf{X} , respectively. The operator $\text{diag}(\cdot)$ has two meanings: When the argument is a matrix, it takes the diagonal elements and puts them into a column

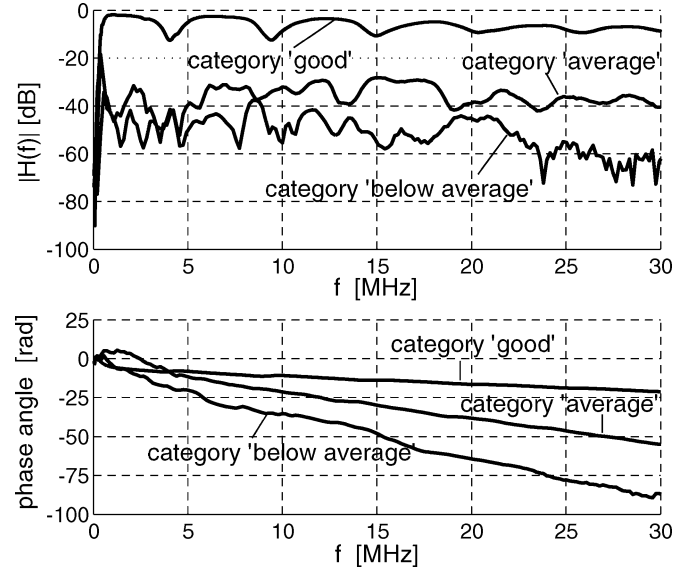


Fig. 2. Transfer functions of three measured PLC channels.

vector. When the argument is a vector, it puts the elements of the vector into a diagonal matrix.

II. PLC MEASUREMENTS

To determine the characteristic properties of indoor low-voltage system PLC channels, measured transfer functions and measured noise power density spectrum (PDS) of the channels are used. Transfer functions are measured by a network analyzer, noise PDS by a spectrum analyzer. Couplers are used to connect the measurement devices to the power line. Additional information about PLC measurements and the properties of PLC channels can be found, e.g., in [1] and [12]–[18]. In the following, we review some properties of indoor PLC channels that are needed in the remaining part of this paper.

In our measurements, the transfer functions show high differences regarding the frequency-selectivity and the average attenuation—which are typical for indoor PLC channels (see the above mentioned references). Fig. 2 shows three examples of measured PLC transfer functions, roughly classified according to the average attenuation in the categories “good,” “average,” and “below average.” The PLC channels in one room (or in adjacent rooms) usually belong to the categories “good” or “average.” In our measurement campaign, “below average” PLC channels are typically found in case of connections between not adjacent rooms; therefore, they do not match the scenario shown in Fig. 1, and we will treat them as worst case situations for our considerations. The characteristics of PLC transfer functions depend on different factors: the cable length of the power line between the two power outlets that define entry and exit point of the PLC channel, the included phase conductors and fuse circuits, and multipath propagation because of reflections (Fig. 3).

Such reflections are generated, e.g., at open-ended power outlets or at devices connected to the power line with their loads not matched to the frequency-dependent impedance of the power line network (cf. [17]). Fig. 4 shows an example of the variations within 8 h of the amplitude spectrum of a measured PLC transfer functions. According to our measurements, the transfer

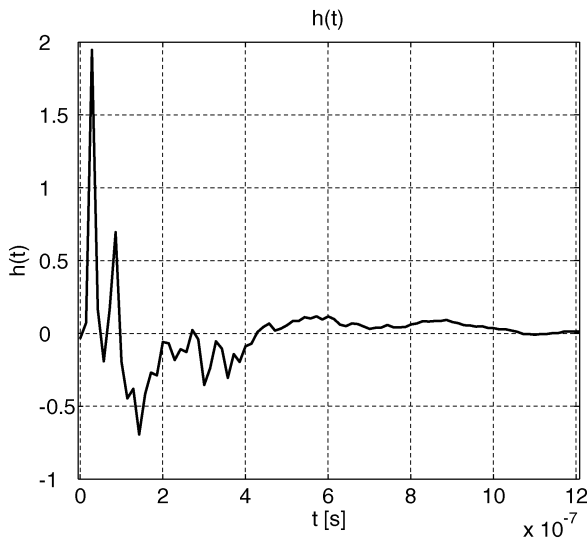


Fig. 3. Impulse response of a PLC channel (category “good”).

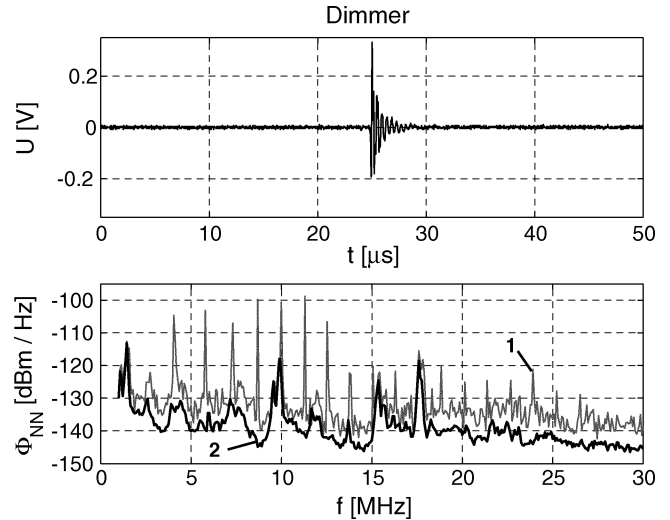


Fig. 5. Part of periodical time function of a dimmer and measured noise power delay spectrum of a PLC channel with a dimmer (1) and without (2).

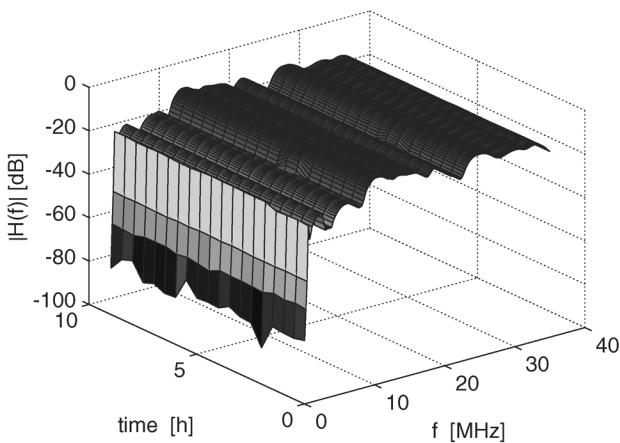


Fig. 4. Variations over time (8 h) of the amplitude spectrum of a PLC transfer function.

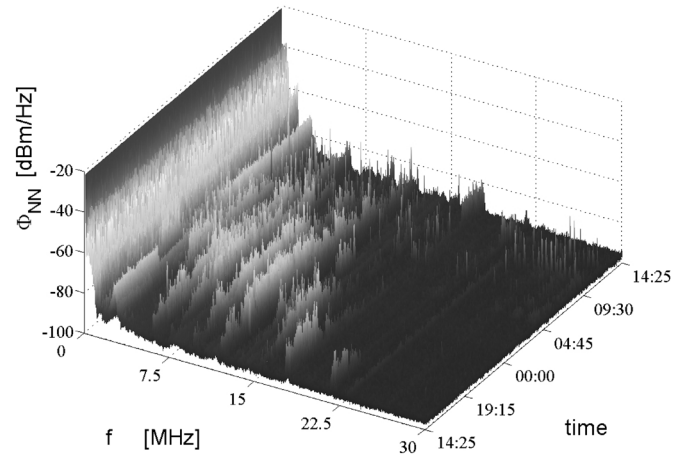


Fig. 6. Variations over time (24 h) of a measured noise PDS of a PLC channel.

functions of PLC channels vary only slowly over time except for modifications of the power line topology next to the considered PLC channel, e.g., in case a device is plugged in. In many cases, PLC channels seem even to be quasi-static, usually their frequency response is at least less variant than the transfer function of a wireless channel between mobile nodes. But in literature (e.g., [19]), cases are reported where PLC channels are highly time-variant, in particular, when devices with time-variant impedances are in the neighborhood of the considered PLC channel.

In Figs. 5 and 6, noise measurements for PLC channels are shown. The use of electrical devices is one reason for noise at the power line (Fig. 5 shows the influence of a dimmer as an example). Other reasons are narrowband interferers—e.g., (medium/short wave) radio transmitter and radio stations. Curve 2 in the lower part of Fig. 5 shows a typical noise PDS of a PLC channel. Distinct narrowband interferences can be found.

In Fig. 6, the variations of the PDS within 24 h is shown. All in all, it can be seen that transfer function and PDS of a

PLC channel are frequency-selective, strongly depending on the location and vary only slowly over time; in addition, impulsive noise can be expected (upper part of Fig. 5). In the following, we model the influence of impulsive noise by its spectral behavior.

A. Channel Capacity

In Europe, the maximum permitted radiation for unshielded cables is restricted by standards (because of EMC reasons). In this paper, a low transmit power density of $\Phi_{TT}(f) = 1.38e - 8 V^2/Hz$ (constant for the considered bandwidth B) is assumed, that meets—according to [12]—the regulations of the NB 30 [22] specified by German national regulatory authorities and, e.g., also applied in Switzerland to limit the interference of PLC devices on other services [23]. This power density corresponds to a transmit power of 8 mW at 50Ω and a bandwidth of $B = 29 \text{ MHz}$ (1 MHz, . . . , 30 MHz).

To approximate the capacity of a channel, a measured transfer function and a measured noise PDS are used. The channel is divided into N narrowband flat-fading subchannels of bandwidth

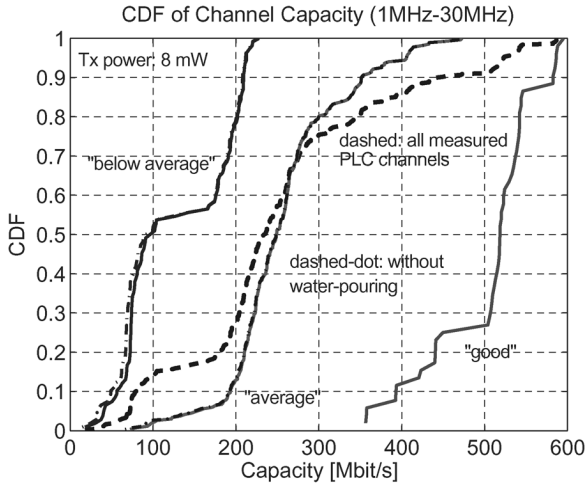


Fig. 7. Measured PLC channels: cumulative distribution function of channel capacity for the different categories; dashed-dotted: without water-filling, uniformly distributed transmit power; dashed: all PLC channels regardless of category.

$\Delta f = B/N$, where N is the number of samples of the measured transfer function $H(k\Delta f)$ and of the measured noise PDS $\Phi_{NN}(k\Delta f)$

$$C \approx \Delta f \cdot \sum_{k=1}^N \log_2 \left(1 + \frac{\Phi_{TT}(k\Delta f) \cdot |H(k\Delta f)|^2}{\Phi_{NN}(k\Delta f)} \right). \quad (1)$$

The noise of each subchannel k is approximated as additive white Gaussian noise (AWGN) of variance $\sigma_k^2 = \Phi_{NN}(k\Delta f) \cdot \Delta f$. The samples of the power density of the transmitted signal $\Phi_{TT}(k\Delta f)$ are found using water-pouring.

Fig. 7 shows the cumulative distribution functions (CDFs) of the channel capacity of 430 measured PLC channels. The dashed curve shows the CDF for all measured channels, the other three curves show the CDFs of the three categories for the transfer functions. Dashed-dotted curves are showing the CDF for the cases where water-pouring is not used but the transmit power is uniformly distributed over frequency. A (small) difference can only be seen in the case of the “below average” PLC channels, because of the low signal-to-noise ratio (SNR) for this channel category. Obviously, channel capacities of more than 400 Mbit/s are not rare even at the low transmit power density that is considered. More than 70% of all measured PLC channels have a capacity of more than 200 Mbit/s (but it should be noted that a large share of the channels are characterized by short distances because they are measured in the same room or in adjacent rooms; this may explain the lower capacity values found in some other published measurement campaigns); even in the category “below average” there are only 3% of the channels with less than 38 Mbit/s capacity.

III. WIRELESS MULTIUSER ZERO-FORCING RELAYING (MU-ZFR)

Shortly, we review the MU-ZFR scheme presented in [7] and show its robustness with respect to noisy CSI and phase noise at the local oscillators. To this end, consider Fig. 1. It depicts a

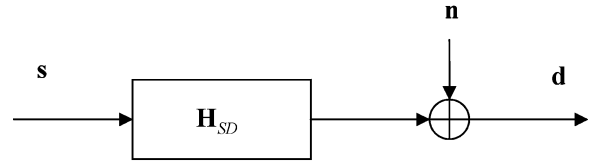


Fig. 8. MU-ZFR equivalent channel model.

scenario where $N_a = 2$ source/destination pairs shall communicate with the assistance of $N_r = 3$ AF (also called “nonregenerative”) relays. All nodes in the network are assumed to utilize a single-antenna only. The communication follows a two-hop relay traffic pattern, i.e., each transmission cycle includes two time slots: In the first time slot, all sources transmit their data to the relays. There, the samples are scaled and rotated, i.e., multiplied with complex gain factors. In the second time slot, the relays forward their signals to all destinations. The complex gain factors at the relaying terminals are calculated such that the transmit data of source node i is received by destination i without interference from other sources (MU-ZFR). Consider the equivalent system model in Fig. 8. For one OFDM subcarrier, the transmit symbols of all sources are stacked in the vector $\mathbf{s} \in \mathbb{C}^{N_a}$, and the received symbols at all destinations in the vector $\mathbf{d} \in \mathbb{C}^{N_a}$. The equivalent channel matrix $\mathbf{H}_{SD} \in \mathbb{C}^{N_a \times N_a}$ is the concatenation of the source-relay channel matrix \mathbf{H}_{SR} , the relay gain factors, and the relay-destination channel matrix \mathbf{H}_{RD} . Finally, the vector $\mathbf{n} \in \mathbb{C}^{N_a}$ contains the noise that is present at the destinations. It consists of the noise at the relays, which is transmitted to the destinations, as well as the noise contributions at the destinations themselves.

Let $\mathbf{h}_{SR}^{(k)}$ denote the vector of channel coefficients from the source k to all relays and $\mathbf{h}_{RD}^{(m)}$ the vector of channel coefficients from all relays to destination m . The entries of the equivalent channel matrix can be written as

$$\mathbf{H}_{SD}[m, k] = \mathbf{g}^H \cdot \left(\mathbf{h}_{RD}^{(m)} \odot \mathbf{h}_{SR}^{(k)} \right) \forall k, m \in \{1, \dots, N_a\} \quad (2)$$

where the vector \mathbf{g} contains the N_r complex-valued relay gain factors. We define a matrix of interference coefficients with its i columns ($i = 1, \dots, N_a \cdot (N_a - 1)$) according to

$$\mathbf{H}[:, i] = \mathbf{h}_{RD}^{(m)} \odot \mathbf{h}_{SR}^{(k)} \forall k, m \in \{1, \dots, N_a\} \text{ and } k \neq m. \quad (3)$$

The interference between different source/destination links is nulled, if the relay gain vector \mathbf{g} satisfies [7] $\mathbf{g}^H \cdot \mathbf{H} \equiv \mathbf{0}$. In this case, the equivalent channel matrix \mathbf{H}_{SD} becomes diagonal. In order to find such a gain vector, we choose an initial gain vector $\mathbf{g}_{\text{init}} = \text{diag}(\mathbf{H}_{SR}^* \mathbf{H}_{RD}^*)$ which would orthogonalize the links for asymptotic number of relays [7] and project it onto the null space of \mathbf{H}

$$\mathbf{g}_{\text{ZF}} = \mathbf{Z} \mathbf{Z}^H \cdot \mathbf{g}_{\text{init}}, \text{ where } \mathbf{Z} = \text{null}(\mathbf{H}^H). \quad (4)$$

At least $N_a \cdot (N_a - 1) + 1$ relays are needed in order to perform the nullspace projection (4), because the nullspace of \mathbf{H} might

be empty for $N_r < N_a \cdot (N_a - 1) + 1$. We denote the case that $N_r = N_a \cdot (N_a - 1) + 1$, which consequently is the minimum number of relays needed to completely orthogonalize all links, by *minimum relay configuration*. In a practical system, where the number of relays is less than that, a scheduling algorithm could orthogonalize sets of $N'_a \leq (1 + \sqrt{1 - 4(1 - N_r)})/2$ source/destination pairs in time. The relays would then be able to orthogonalize each of the sets at a time. Compared with the case where enough relays are present to orthogonalize all links simultaneously, the sum rate would decrease because more time slots are needed for one transmission cycle.

In order to find their zero-forcing gain factors locally, each relay needs to know \mathbf{H}_{SR} and \mathbf{H}_{RD} perfectly, i.e., it needs to have *global channel knowledge*. In addition to that, all relays have to be phase synchronous in order to accomplish coherent combining at the destinations.

MU-ZFR allows all source/destination pairs to communicate in parallel over the same physical channel, which essentially realizes a distributed spatial multiplexing gain. As a measure of performance of the present system, we choose the *average sum rate*, which is given by

$$I_{\text{avg}} = \frac{1}{2} E_{\{\mathbf{H}_{SD}\}} [I_{\text{sum}}] = \frac{1}{2} E_{\{\mathbf{H}_{SD}\}} \left[\sum_{k=1}^{N_a} \log_2 (1 + \rho_k(\mathbf{H}_{SD})) \right] \quad (5)$$

where $\rho_k(\mathbf{H}_{SD})$ denotes the instantaneous signal-to-interference-noise ratio (SINR) of source/destination pair k for a given channel realization. The factor 1/2 accounts for the fact that a transmission occupies two channel uses as it needs two time slots.

In the following, we show the performance of MU-ZFR in terms of average achievable rates in bits per second per Hertz. Further, we discuss the robustness of MU-ZFR with respect to two main error sources: 1) noisy CSI due to channel estimation and quantization of the channel estimates before feedback and 2) the influence of errors in the phase of the local oscillators of the distributed relays due to phase noise. From this, we can derive requirements to the PLC backbone. Fig. 9 shows the average sum rate I_{avg} of a minimum relay configuration versus the number of source/destination pairs. The parameter of the curves is the average SNR. In order to have a defined average SNR at each destination, we consider a reference scenario with a single source/destination pair and only one relay in between. From this, we determine the transmit power σ_s^2 of source and relay which is needed to achieve this defined *reference SNR*. For the MU-ZFR scenario, we apply this transmit power to the configuration that is to be evaluated. Thus, each source has transmit power σ_s^2 , whereas all relays share the sum transmit power of $N_a \cdot \sigma_s^2$. Further, it is assumed that relays and destinations have same noise variances. For the simulations, we assumed frequency flat Rayleigh fading on every single source-relay and relay-destination link. All channel coefficients are statistically independent and drawn from a complex normal distribution with zero-mean and variance 1. The channel matrices \mathbf{H}_{SR} and \mathbf{H}_{RD} are constant during each transmission cycle

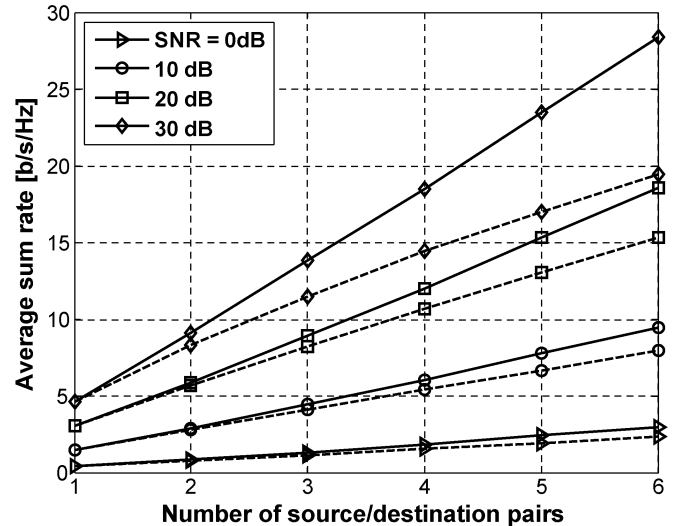


Fig. 9. Average sum rate versus number of source/destination pairs for perfect CSI and synchronization (solid lines) and estimated CSI with processing gain of 10 dB and Gaussian distributed phase jitter of 2° rms (dashed lines). Parameter of the curve is the defined SNR.

(block fading) and temporally independent. All relays are assumed to exhibit the same noise variance, as do all the destinations.

The potential of MU-ZFR within a distributed network can be easily seen in Fig. 9. For perfect CSI and synchronization (solid lines), the average sum rate increases linearly with the number of source/destination pairs which exhibit the achieved distributed spatial multiplexing gain. However, imperfections due to noisy CSI and synchronization have the effect that the sum rate no longer increases linearly but saturates (dashed lines: exemplary values for synchronization and channel estimation imperfections) [11].

To visualize the effect of noisy CSI and synchronization errors, we plot the average rate per link versus imperfections for $N_a = 3$ source/destination pairs. In Fig. 10, the average per link rate versus SNR_{CSI} (excess SNR of the channel estimate relative to the defined reference SNR) is shown. Parameter of the curves is the reference SNR. The error is modeled by a complex Gaussian noise added to the exact channel matrices. It can be seen that the rates are nearly unaffected by the noisy CSI for a SNR_{CSI} larger than 10 dB. Already for an excess SNR of 5 dB, the loss in spectral efficiency is quite small.

Fig. 11 depicts the influence of an additive Gaussian error of the reference phase at all relays on the average rate per link for $N_a = 3$ source/destination pairs. It can be seen that for increasing reference SNR the negative influence of the phase jitter also increases. The phase jitter causes a residual noise variance at the destinations which limits the average rates.

IV. PLC BACKBONE FOR WIRELESS RELAYING

A. Wireless MU-ZFR: Relay Initialization and Updates of CSI

In the initialization phase of wireless MU-ZFR, every relay broadcasts its CSI regarding the wireless source/destination nodes to all other relays using the power line. Each of the N_r relays has to estimate $2N_a$ complex channel taps per OFDM

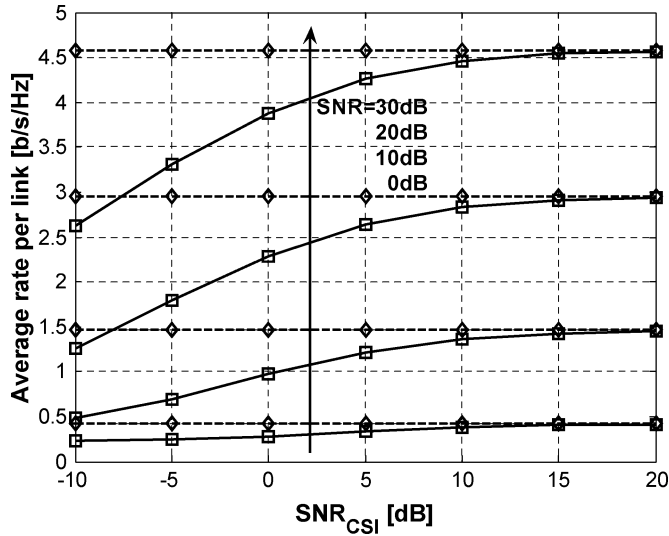


Fig. 10. Average per link rate versus excess SNR of channel estimate compared with defined reference SNR (solid lines). Parameter of the curves is reference SNR. The dashed lines depict achievable rates for perfect CSI. $N_a = 3$.

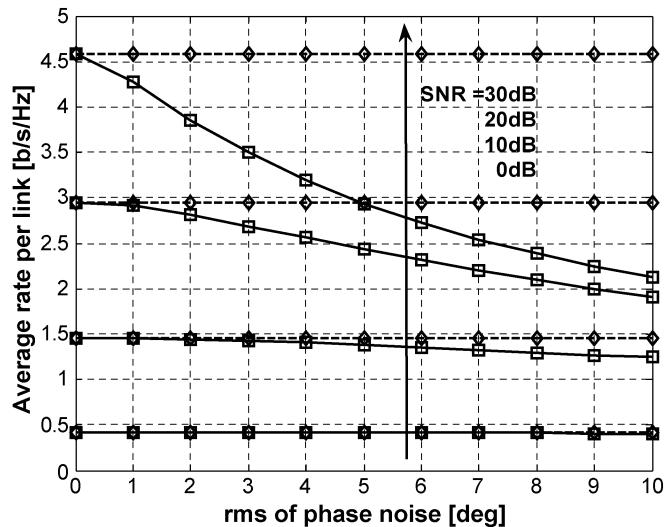


Fig. 11. Average rate per link versus rms of a Gaussian phase jitter (solid lines). Parameter of the curves is reference SNR. The dashed lines depict achievable rates for perfect phase synchronization. $N_a = 3$.

subcarrier (one uplink and one downlink tap per source/destination pair). We assume 8 bytes per complex channel tap, including coding for error protection. Each relay broadcasts this estimated CSI to all other relays using PLC. If a relay does not receive the CSI of all other relays, a protocol scheme is assumed that reduces the number of assisting relays to these relays that have all CSI of each other. The data transmitted over PLC adds up to $16 N_r N_a$ bytes.

We consider the following example: number of wireless source/destination pairs $N_a = 3$; number of relays $N_r = 10$, update of CSI every 10 ms. This leads to a sum data rate of 48 kByte/s = 0.384 Mbit/s. If the wireless source/destination nodes use 128 OFDM subcarriers, and if the channel taps of every subcarrier has to be transmitted (usually it is enough to transmit much less—depending on the resolvable channel paths), the (maximum) sum rate for PLC is 49.152 Mbit/s. Be-

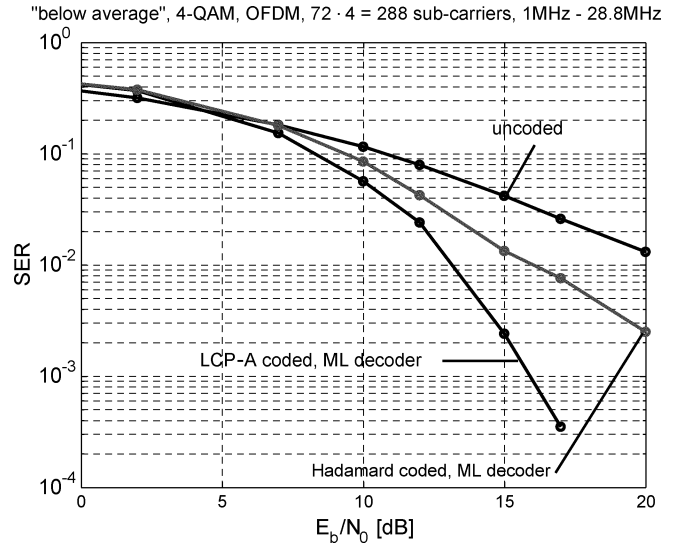


Fig. 12. SER performance: OFDM, 4-QAM, channel "below average," encoder block length 4, ML decoder.

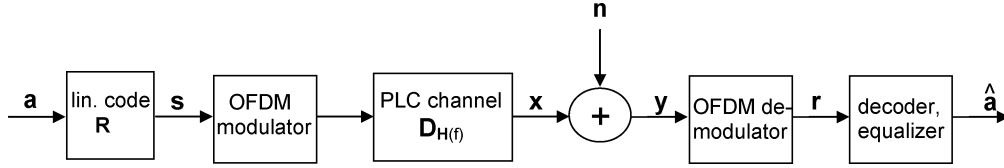
cause the information is broadcasted between the relays, every PLC channel between two relays has to support this sum rate. This inter-relay-communication enables much higher data rates on the wireless medium by allowing multiple simultaneous connections without mutual interference.

As Fig. 7 shows, for more than 98% of all measured PLC channels, the channel capacity is higher than 50 Mbit/s; even in the category "below average" there are more than 92% with a capacity high enough to support the necessary data rate. For $N_r = 10$ relays, there are $\binom{10}{2} = 45$ different PLC channels. In the considered example there is a high probability that none of the 45 channels is affected. Even if one channel fails, nine relays remain (not eight) because if a link between two relays does not support the rate, then it is enough that one of these relays does not assist the communication between the wireless sources and destination nodes. The remaining nine relays are enough to enable MU-ZFR because at least seven relays are necessary to support three source/destination pairs [7], [10].

B. PLC Transmission Scheme

Because the channels are highly frequency-selective, OFDM is suitable for PLC (see, e.g., [24]). In addition, for OFDM, it is possible to leave particular frequencies unused, e.g., because of high attenuation/disturbances or due to EMC reasons; furthermore, the relays use OFDM for the wireless communications. Our measurements show durations of the channel impulse response of up to 3 μ s (in category "below average"); i.e., the OFDM guard time should be at least 3 μ s. So, an OFDM symbol duration of at least 10 μ s ($\Delta f_{sc} = 100$ kHz subcarrier spacing) seems appropriate and is used exemplarily in the following (although an increase of the OFDM symbol duration would decrease the overhead due to the guard interval).

As an example, we consider $N = 288$ OFDM subcarriers with 100 kHz spacing (frequency range 1 MHz, ..., 28.8 MHz). Fig. 12 shows the symbol error rate (SER) versus receiver SNR for uncoded OFDM transmission—4-QAM on all subcarriers—over the "below average" channel shown in Fig. 2. A


 Fig. 13. OFDM system with linear precoding matrix \mathbf{R} .

measured noise PDS of this channel is used to generate colored noise; perfect CSI is assumed at the receiver; 20 dB receive SNR corresponds for this PLC channel to about 2.3 mW transmit power. For this value, the uncoded OFDM achieves almost a symbol error rate of $\text{SER} = 1e - 2$. To improve the SER performance, a coding scheme is suitable that exploits the frequency diversity of the channel, because it is not possible to increase the transmit power above a limit given by regulations for PLC. In environments where the PLC channel is quasi-static, precoding schemes at the transmitter using *a priori* CSI could be considered for peer-to-peer transmissions; but we are considering broadcasting between all relays, therefore, these schemes are not feasible, because it is not possible for one relay to adapt to all channels of the other relays.

Our approach is linear precoding using unitary matrices (as shown in Fig. 13); the linear code \mathbf{R} picks up the available frequency diversity without utilizing CSI at the transmitter; it introduces intersymbol interference (ISI) in the presence of fading, therefore, ISI compensation (equalization) at the receiver is needed. A forward error correction (FEC) code in addition to the linear precoder can be used to protect against impulsive noise on the power line; to apply FEC coding instead of the linear precoding for exploiting frequency diversity weakens this noise protection. In the following, we analyze the frequency diversity gain of linear precoding matrices based on the pairwise error probability (PEP); the coding is done across N OFDM subcarriers. Using the Chernoff bound, the PEP can be approximated as

$$P(\mathbf{a}^{(1)} \rightarrow \mathbf{a}^{(2)} | \mathbf{D}_H) \leq \exp\left(-d^2(\mathbf{x}^{(1)}, \mathbf{x}^{(2)}) / 4N_0\right). \quad (6)$$

The $(N \times 1)$ vector \mathbf{x} is the product of the transmit symbol vector \mathbf{s} and the diagonal channel matrix \mathbf{D}_H ; \mathbf{s} is the product of the input symbol vector \mathbf{a} (from an arbitrary symbol alphabet, e.g., 4-QAM) and the linear precoding matrix \mathbf{R} ; \mathbf{D}_H is a $(N \times N)$ diagonal matrix; on the main diagonal are the values of the channel transfer function $H(f)$ corresponding to the N OFDM subcarriers. The Euclidean distance between the vectors $\mathbf{x}^{(1)}$ and $\mathbf{x}^{(2)}$ is referred to as $d^2(\mathbf{x}^{(1)}, \mathbf{x}^{(2)})$; $N_0/2$ is the AWGN variance per dimension (the frequency-selective PLC noise is whitened in the decoder by a whitening filter that takes the noise PDS of the PLC channel into account).

For a certain frequency f , the value of the transfer function $H(f)$ is a random variable resulting from the superposition of numerous independent random variables representing the effects of multipath propagation because of mismatched lines in power line networks [20]. Therefore, according to [20] and [21], the PLC channel can be roughly modeled as Rayleigh fading. If

we assume that the elements of \mathbf{D}_H are independent identically distributed (i.i.d.) zero-mean complex Gaussian with unit energy, then the PEP after averaging with respect to \mathbf{D}_H is given by

$$P(\mathbf{a}^{(1)} \rightarrow \mathbf{a}^{(2)}) \leq \prod_{k=1}^N \left(1 + |\Delta \mathbf{s}[k]|^2 / (4N_0)\right)^{-1}. \quad (7)$$

The differences $\Delta \mathbf{s}[k]$ are the elements of the vector $\Delta \mathbf{s} = \mathbf{s}^{(1)} - \mathbf{s}^{(2)}$ for the dimensions k ($1 \leq k \leq N$). The assumption $|\Delta \mathbf{s}[k]|^2 / (4N_0) \gg 1$ is asymptotically (with increasing SNR) valid if

$$\Delta \mathbf{s}[k] = \mathbf{s}^{(1)}[k] - \mathbf{s}^{(2)}[k] \neq 0. \quad (8)$$

If this inequality holds for M out of the N dimensions, we get asymptotically

$$P(\mathbf{a}^{(1)} \rightarrow \mathbf{a}^{(2)}) \leq (4N_0)^M \cdot \prod_{k=1}^M \left(|\Delta \mathbf{s}[k]|^2\right)^{-1}. \quad (9)$$

The frequency *diversity gain* is given by M , the *coding gain* is

$$G = \prod_{k=1}^M \left(|\Delta \mathbf{s}[k]|^2\right)^{1/M}. \quad (10)$$

As precoding matrix \mathbf{R} , we consider the following three matrices: a Hadamard matrix (e.g., as in [25]), a LCP-A matrix defined in [26], and a Chirp matrix (described as outer code in [27]). Hadamard and LCP-A matrix are only defined for block lengths $N = 2^n$, $n \in \mathbb{N}$; the chirp matrix can be constructed for every block length.

As shown in [26] and [27], for LCP-A and Chirp matrices inequality (8) is valid in all N dimensions for all possible pairs $\mathbf{s}^{(1)}$, $\mathbf{s}^{(2)}$ (with $\mathbf{s}^{(1)} \neq \mathbf{s}^{(2)}$) of a given symbol alphabet; therefore, both precoding matrices are able to achieve the *full frequency diversity gain*; as shown in [26] and [27], the LCP-A codes achieve the optimum coding gain for all block lengths for which these codes are defined. In contrast, for Hadamard matrices the inequality holds only for some pairs $\mathbf{s}^{(1)}$, $\mathbf{s}^{(2)}$ ($\mathbf{s}^{(1)} \neq \mathbf{s}^{(2)}$); for the other pairs the diversity gain is reduced. For 4-QAM and a (4×4) Hadamard precoding matrix, only 80.5% of all possible pairs achieve the full diversity gain, for (8×8) about 91.5%.

These differences regarding the diversity gain are reflected in the simulation results shown in Figs. 12, 14, and 15 (in all simulations, no FEC is used, and perfect CSI at the receiver is assumed). Fig. 12 depicts the gain in SER performance for the

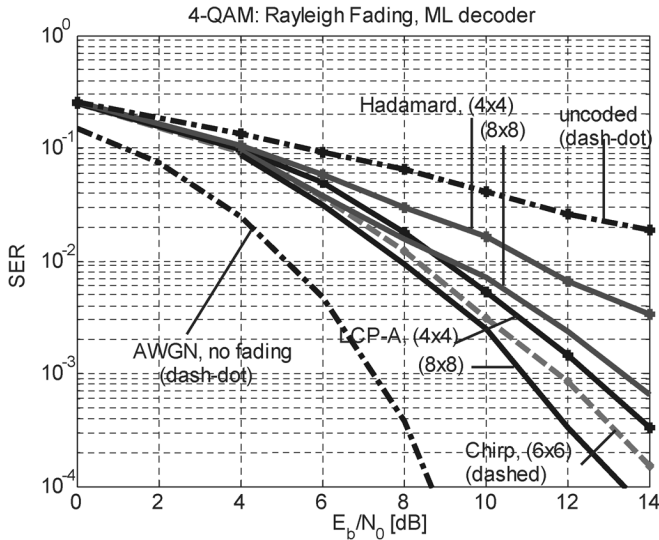


Fig. 14. SER performance: 4-QAM, Rayleigh fading, sphere decoder.

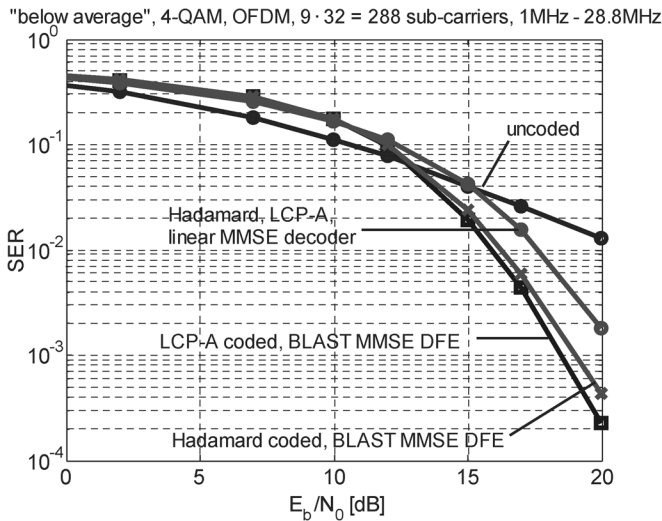


Fig. 15. SER performance: OFDM, 4-QAM, channel “below average,” encoder block length 32, different decoders.

“below average” channel that is available using maximum-likelihood (ML) decoding in combination with a (4×4) LCP-A and a (4×4) Hadamard matrix, respectively. The coding is done across four different, not adjacent (i.e., frequency interleaving) OFDM subcarriers; in this way, 72 coded blocks are transmitted in parallel over the 288 subcarriers in the considered bandwidth. Even for such a small block length ($N = 4$), the diversity gain on the considered PLC channel is high. Fig. 14 shows the performance of different linear precoding matrices in Rayleigh fading for ML decoding and block length $N = 4, 6, 8$. The results show the better performance of the Chirp and the LCP-A matrices compared with the Hadamard matrices—the (6×6) Chirp matrix performs better than the (8×8) Hadamard matrix.

For the simulation results in Fig. 15, a higher code block length is used over the “below average” PLC channel; we divided 288 symbols (one per subcarrier) in 9 blocks with 32 symbols and used a (32×32) Hadamard precoding matrix and a (32×32) LCP-A matrix according to [26], which is known

to achieve the full frequency diversity gain. As stated before, at the receiver, an interference compensation technique has to be used, because the channel fading in combination with the precoding matrices introduces ISI [26]; for the simulations in Fig. 15, we used a BLAST minimum mean-square error-decision feedback equalizer (MMSE-DFE) [28] and a linear MMSE equalizer; because of the block length $N = 32$, the complexity of a ML decoder would be too high. Even with these suboptimal decoders, the SER is much lower than in the case of uncoded OFDM. A variety of different decoders can be used; there is a rich tradeoff between performance and decoder complexity. Whereas for the MMSE equalizer both precoding matrices show comparable SER results, the LCP-A matrix achieves the best performance for the BLAST MMSE-DFE: $\text{SER} = 2e - 4$ for 2.3 mW at a data rate of 57.6 Mbit/s (4-QAM is used for all simulations). Considering the $3 \mu\text{s}$ guard time, the data rate still amounts to 40.32 Mbit/s, which can be increased further by using a higher symbol alphabet (e.g., 16-QAM)—at least for the channels of the categories “average” and “good.” This achievable rate is more than enough for the communication between two relays, even connecting a relay as AP to a backhaul (as shown in Fig. 1) seems feasible.

C. Synchronization of Wireless Relays Over PLC

Now, we investigate, if the PLC OFDM can be used to assist the synchronization process of the relays; the synchronization is necessary to enable a coherent combining of the (wireless) signals that arrive from the relays at the destination nodes. Usually, carrier synchronization in an OFDM system is accomplished by locking on an unmodulated carrier which is used as a pilot tone. The phase of a local oscillator can be derived from the received signal by a phase locked loop (PLL); the local oscillator has an average frequency exactly equal to that of the radio frequency (RF) carrier. A second-order loop can be used to eliminate a constant phase offset. Therefore, we use a zero-mean stationary random process with variance σ_ϕ^2 as a model for the remaining carrier phase jitter (see [29]–[31]). According to [29], the jitter variance at sufficiently high SNR is given by

$$\sigma_\phi^2 \sim N/S \cdot B_N/W \quad (11)$$

W is the signal bandwidth, and B_N the one-sided noise bandwidth of the loop used in synchronization (PLL).

In Fig. 16, the CDFs of the SNR values of all OFDM subcarriers for all measured PLC channels and for all channels in the three categories are given (transmit power 8 mW). More than 20% of all OFDM subcarriers show a SNR value of less than 12 dB (the “below average” channels even lower than 0 dB)—according to [29], 12 dB SNR translates in a worst case approximation to a relatively high jitter variance $\sigma_\phi^2 \approx -15$ dB, which corresponds to about 10° rms phase jitter. As Fig. 11 shows, this leads to a strong degradation of the performance of MU-ZFR.

But in Fig. 17 is shown that more than 98% of the PLC channels show at least one OFDM subcarrier with more than 20 dB SNR; even in the category “below average” for more than 96% the SNR is at least 20 dB. If these subcarriers can

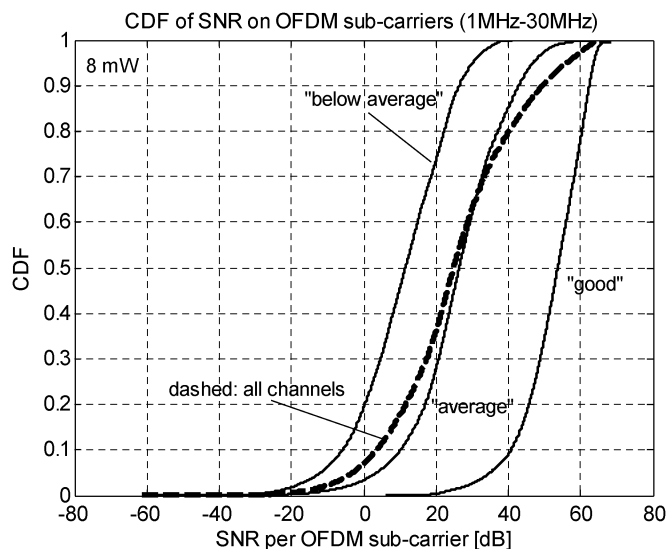


Fig. 16. Measured PLC channels: CDF of SNR per OFDM subcarrier.

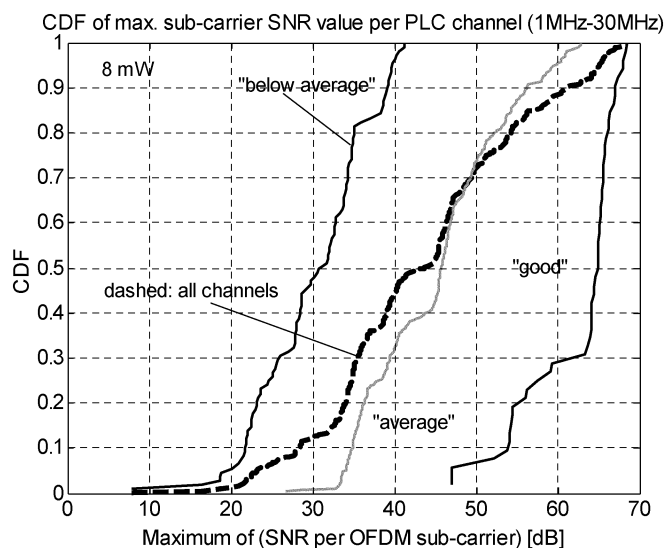


Fig. 17. CDF of maximum SNR values; for every PLC channel only the OFDM subcarrier with highest SNR is considered.

be used as pilot tones for synchronization, the jitter variance is low—approximately $\sigma_\phi^2 \approx -23$ dB in a worst case approximation [29], corresponding to about 4° rms. In this case, MU-ZFR still shows a good performance for three source/destination pairs and a reference SNR between 10 and 20 dB per user—which we consider in this paper as suitable operating point for MU-ZFR. Because of system imperfections the use of only three or four users seems to be a good compromise between performance and complexity. Therefore, the relays can use a pilot tone in the PLC OFDM to establish a synchronization of the symbol timing; if the jitter is low and very narrow PLL filters are used, then even the wireless carrier phase synchronization can be assisted by the PLC reference signal directly.

V. CONCLUSION

In this paper, we study the feasibility of using PLC to assist cooperative wireless relaying. As an example, we consider

wireless MU-ZFR, which enables high data rates on the wireless medium by exploiting distributed spatial multiplexing; this scheme causes a considerable high data exchange between the relays for synchronization, initialization and CSI updates. The key idea is to use PLC for this overhead. Based on a measurement campaign of indoor PLC channels, we analyze properties of the PLC channel and propose a precoded OFDM transmission scheme; this scheme can be used for synchronization and inter-relay-communication over power line, even using low transmit power to meet given regulations.

We conclude that PLC is a promising candidate to enhance wireless relaying schemes that are based on inter-relay-communication: The channel capacity of typical indoor PLC channels is high enough to deal with data rates necessary for the inter-relay communication; the expected SNRs allow for low jitter; the precoded OFDM transmission scheme exploits the frequency-diversity of PLC channels optimally with reasonable and scalable decoder complexity. Using PLC, the overhead due to the inter-relay-communication does not affect the wireless part, costs are reduced because additional wiring is not needed, and relays can be plugged in wherever needed.

REFERENCES

- [1] M. Gebhardt, F. Weinmann, and K. Dostert, "Physical and regulatory constraints for communication over the power supply grid," *IEEE Commun. Mag.*, vol. 41, no. 5, May 2003.
- [2] *Proc. IEEE Special Issue on Gigabit Wireless*, vol. 92, no. 2, Feb. 2004.
- [3] N. Laneman, D. Tse, and G. Wornell, "Cooperative diversity in wireless networks: Efficient protocols and outage behavior," *IEEE Trans. Inf. Theory*, vol. 50, pp. 3062–3080, Dec. 2004.
- [4] A. Sendonaris, E. Erkip, and B. Aazhang, "User cooperation diversity—Part I and II," *IEEE Trans. Commun.*, pp. 1927–1948, Nov. 2003.
- [5] I. Hammerström, M. Kuhn, and A. Wittneben, "Cooperative diversity by relay phase rotations in block fading environments," in *Proc. IEEE Workshop Signal Process. Advances Wireless Commun.*, Jul. 2004, pp. 293–297.
- [6] R. U. Nabar, O. Oyman, H. Bölcskei, and A. Paulraj, "Capacity scaling laws in MIMO wireless networks," in *Proc. Allerton Conf. Commun., Control and Comp.*, Oct. 2003, pp. 378–389.
- [7] A. Wittneben and B. Rankov, "Distributed antenna systems and linear relaying for gigabit MIMO wireless," in *Proc. IEEE Veh. Technol. Conf.-Fall*, Los Angeles, CA, Sep. 2004, pp. 3624–3630.
- [8] M. Kuhn and A. Wittneben, "Wireless relaying with partial cooperation based on power-line communication," in *Proc. IEEE Workshop Signal Process. Advances Wireless Commun.*, New York, Jun. 2005, pp. 590–594.
- [9] L. Lampe, R. Schober, and S. Yiu, "Multihop transmission in power line communication networks: Analysis and distributed space-time coding," in *Proc. IEEE Workshop Signal Process. Advances Wireless Commun.*, New York, Jun. 2005, pp. 1006–1012.
- [10] A. Wittneben and I. Hammerström, "Multiuser zero forcing relaying with noisy channel state information," in *Proc. IEEE Wireless Commun. Netw. Conf.*, Mar. 2005, pp. 1018–1023.
- [11] A. Wittneben, "A theoretical analysis of multiuser zero forcing relaying with noisy channel state information," in *Proc. IEEE Veh. Technol. Conf.-Spring*, Stockholm, Sweden, Sep. 2005, pp. 1509–1513.
- [12] M. Götz, M. Rapp, and K. Dostert, "Power line channel characteristics and their effect on communications system design," *IEEE Commun. Mag.*, pp. 78–86, Apr. 2004.
- [13] D. Anastasiadou and T. Antonakopoulos, "Multipath characterization of indoor power-line networks," *IEEE Trans. Power Del.*, vol. 20, no. 1, pp. 90–99, Jan. 2005.
- [14] D. Liu, E. Flint, B. Gaucher, and Y. Kwark, "Wide band AC power line characterization," *IEEE Trans. Consum. Electron.*, vol. 45, no. 4, pp. 1087–1097, Nov. 1994.
- [15] L. T. Tang, P. L. So, E. Gunawan, Y. L. Guan, S. Chen, and T. T. Lie, "Characterization and modeling of in-building power lines for high-speed data transmission," *IEEE Trans. Power Del.*, vol. 18, no. 1, pp. 69–77, Jan. 2003.

- [16] H. Philipps, "Performance measurements of powerline channels at high frequencies," in *Proc. 2nd Int. Symp. Power Line Commun. Appl.*, 1998, pp. 229–237.
- [17] M. Zimmermann and K. Dostert, "A multipath model for the powerline channel," *IEEE Trans. Commun.*, vol. 50, no. 4, pp. 553–559, Apr. 2002.
- [18] M. Kuhn and A. Wittneben, "PLC enhanced wireless access networks: A link level capacity consideration," in *Proc. IEEE Veh. Technol. Conf.-Spring*, Birmingham, AL, May 2002, pp. 125–129.
- [19] J. A. Cortes, F. J. Canete, and L. Diez, "Characterization of the cyclic short-time variation of indoor power-line channels," in *Proc. Int. Symp. Power Line Commun. Appl.*, Apr. 2005, pp. 326–330.
- [20] L. Lampe and J. B. Huber, "Bandwidth efficient power line communications based on OFDM," *Int. J. Elect. Commun.*, vol. 54, no. 1, pp. 2–12, 2000.
- [21] E. Biglieri, "Coding and modulation for a horrible channel," *IEEE Commun. Mag.*, vol. 41, no. 5, pp. 92–98, May 2003.
- [22] "Annex to the decree on planning allocation of frequency ranges," in *Nutzungsbestimmung 30 (NB 30)*. Germany: RegTP, Jul. 2001. [Online]. Available: <http://www.regtp.de>
- [23] OFCOM, OFCOM technical guide NT-2721—PLC (Powerline Communications) Equipment, Jan. 2005. [Online]. Available: <http://www.bakom.ch>
- [24] E. Del Re, R. Fantacci, S. Morosi, and R. Seravalle, "Comparison of CDMA and OFDM techniques for downstream power-line communications on low voltage grid," *IEEE Trans. Power Del.*, vol. 18, no. 4, pp. 1104–1109, Oct. 2003.
- [25] Y.-P. Lin and S.-M. Phoong, "BER minimized OFDM systems with channel independent precoders," *IEEE Trans. Signal Process.*, vol. 51, no. 9, pp. 2369–2380, Sep. 2003.
- [26] Y. Xin, Z. Wang, and G. B. Giannakis, "Space-time diversity systems based on linear constellation precoding," *IEEE Trans. Wireless Commun.*, vol. 2, no. 2, pp. 294–309, 2003.
- [27] M. Kuhn, I. Hammerstroem, and A. Wittneben, "Linear scalable dispersion codes: Signal design and performance analysis," in *Proc. IEEE Veh. Technol. Conf.-Spring*, May 2004, pp. 838–842.
- [28] G. D. Golden, G. J. Foschini, R. A. Valenuela, and P. W. Wolniansky, "Detection algorithm and initial laboratory results using V- BLAST space-time communication architecture," *Electron. Lett.*, vol. 35, no. 1, pp. 14–16, Jan. 1999.
- [29] L. E. Franks, "Carrier and bit synchronization in data communication—A tutorial review," *IEEE Trans. Commun.*, vol. Com-28, no. 8, pt. 2, pp. 1107–1121, Aug. 1980.
- [30] T. Pollet, M. Moeneclaey, I. Jeanclaude, and H. Sari, "Carrier phase jitter sensitivity for single-carrier and multi-carrier QAM systems," in *Proc. Symp. Commun. Veh. Technol. in the Benelux*, 1994, pp. 174–181.
- [31] H. Steendam and M. Moeneclaey, "Synchronization sensitivity of multicarrier systems," *Eur. Trans. Commun., ETT Special Issue on Multi-Carrier Spread Spectrum*, vol. 15, no. 3, pp. 223–23, May–Jun. 2004.



Marc Kuhn was born in Saarlouis, Germany. He received the Dipl.-Ing. and Dr.-Ing. degrees in electrical engineering from Saarland University, Saarbrücken, Germany, in 1998 and 2002, respectively.

Since 2002, he has been with the Communication Technology Laboratory, Swiss Federal Institute of Technology (ETH) Zurich, Zurich, Switzerland, where he is currently a Senior Researcher. His main research interests are in wireless communications including space–time coding, MIMO communication,

cooperative signal processing, and power line communication.



Stefan Berger was born in Münster, Germany, on June 22, 1978. He received the Dipl.-Ing. degree in electrical engineering from Munich University of Technology, Munich, Germany, in 2003. Since 2003, he has been working towards the Ph.D. degree in electrical engineering at the Communication Technology Laboratory (CTL), Swiss Federal Institute of Technology (ETH) Zurich, Zurich, Switzerland.

His research interests are in the field of distributed wireless ad hoc and sensor networks with special focus on cooperative wireless relaying.



Ingmar Hammerström received the Dipl.-Ing. degree in electrical engineering from RWTH Aachen University, Aachen, Germany, in 2001. Since 2002, he has been working towards the Dr. Sc. degree at the Communication Technology Laboratory (CTL), Swiss Federal Institute of Technology (ETH) Zurich, Zurich, Switzerland.

His research interests are in the field of signal processing for wireless communications including MIMO, space–time coding, cooperative diversity, and adaptive scheduling in ad hoc networks.

Mr. Hammerström received a Best Paper Award at the IEEE Vehicular Technology Conference, Los Angeles, CA, in September 2004.



Armin Wittneben received the Dipl.-Ing. and Ph.D. degrees in electrical engineering from the Technical University Darmstadt (TUD), Darmstadt, Germany, in 1983 and 1989, respectively. In 1997, he completed his habilitation thesis and received the Venia Legendi in Communication Technology from the TUD.

He is Full Professor of Wireless Communication at the Swiss Federal Institute of Technology (ETH) Zurich, Zurich, Switzerland, and Director of the Communication Technology Laboratory. From 1989 to 1998, he was with ASCOM/Switzerland and in charge of the research activities of this company in wireless communications. During this period, the department demonstrated among others the first Hiperlan/I modem and the fastest modem worldwide for digital power line communication. In 1998, he accepted a position as Full Professor of Communications at the Saarland University, Saarbrücken, Germany. In 2002, he joined ETH Zurich. His research work focuses on cooperative wireless communication, communication theory, digital signal processing, MIMO wireless, and ultra-wideband wireless.